ORIGIN MECHANISM OF HERCYNITE-KAMACITE OBJECTS: EVIDENCE FOR LIQUID IMMISCIBILITY PHENOMENA IN THE YAMATO-82133 ORDINARY CHONDRITE (H3)

Nina G. Zinovieva, Olga B. Mitreikina and Lev B. Granovsky

Department of Petrology, Faculty of Geology, Moscow State University,
Lenin Gory, Moscow 119899, Russia

Abstract: Peculiar mineral aggregates detected in the nonequilibrated Yamato-82133 ordinary chondrite (H3) include regular intergrowths of hercynite and kamacite, sometimes with corundum. In addition to hercynite, kamacite, and corundum, the typical minerals of the hercynite-kamacite objects (HKO) are chrome spinels and phosphates (apatite, whitlockite, and a Ca-free Na-K analog of fillowite). HKO are most widespread in the chondrite matrix but also occur in the porphyritic pyroxene-olivine and olivine chondrules, in which HKO were detected in form of droplets. The latter stick together to produce dumbbell-shaped aggregates. Intrachondrule HKO are zoned and have magmatic textures. Their textural relationships and specific mineralogical features are indicative of the magmatic genesis of intrachondrule HKO and provide information on the composition of the parental melt. The textural identity between intrachondrule and matrix HKO and similarities in their mineral assemblages and mineral chemistries suggest their similar genesis.

1. Introduction

The Yamato-82133 ordinary chondrite (H3) is characteristic in having widespread peculiar aggregates: they contain regular intergrowths of hercynite and kamacite, sometimes in association with corundum (Zinovieva *et al.*, 1996b, c). Al-bearing phases (hercynite and corundum) are apparently restricted to certain textural sites and cannot be contaminants. In these aggregates, kamacite strongly dominates over hercynite and, particularly, over corundum, with the two latter minerals developing as triangular aggregates governed by a latticework of fractures (set at angles of 60°) in kamacite (Fig. 1). The hercynite-kamacite objects (HKO) are more widespread in the chondrite matrix but also occur as droplets in the silicate chondrules. The Yamato-82133 meteorite is a heavily oxidized nonequilibrated H3 ordinary chondrite (Yanai and Kojima, 1995). It consists of olivine-pyroxene and pyroxene olivine chondrules with granular, barred, or porphyritic textures, which are cemented by a sulfide-metal matrix containing some amount of silicate material. Silica-pyroxene chondrules with barred or granular textures are rarer. The olivine and pyroxene of most of the chondrules exhibit a normal zoning, which is suggestive of an increasing oxygen activity during the crystallization of the silicate chondrule melt. At the same time, the chondrite bears olivine pyroxene chondrules, in which the silicate zoning grades from reverse to normal (complex zoning), a fact suggesting a sharp drop of the oxidation potential imme-

Fig. 1. Back-scattered electron (BSE) image of the texture of a hercynite-kamacite aggregate. Km–kamacite, Her–hercynite, Tn–taenite; Al–corundum; gray–iron oxides.

diately before the stage of strongly oxidized conditions in the course the chondrule crystallization (ZINOVIEVA *et al.*, 1995).

2. Textures

Hercynite-kamacite aggregates occur in the chondrite matrix interstitially between silicate chondrules (Fig. 2). Sometimes, HKO form veinlets, which intrude chondrules and cut them, or develop as rounded chondrule-like aggregates ranging from 100 to 1500 μm in diameter (Fig. 3), which are clearly separated from the more oxidized metallic matrix. Analogous aggregates are detected in pyroxene-olivine porphyritic chondrules, which show both normal zoning of their silicates and complex varying iron mole fractions of the olivine and pyroxene. HKO occur in porphyritic pyroxene-olivine chondrules as droplets (ranging from a few to a few hundred micrometers) in olivine and pyroxene grains or in their interstices (Fig. 4). In the chondrules, silicate crystals are euhedral with respect to hercynite-kamacite droplets, whose melt crystallized after the silicate melt and, the former was partly squeezed into the interstices between silicate grains. These specific aggregates in chondrules sometimes have a porphyritic texture (Fig. 5), with interstices between relatively large kamacite crystals filled with fine-grained hercynite-kamacite material. The hercynite-kamacite droplets sometimes coalesce into dumbbell-shaped bodies (Fig. 6). The droplets are usually zoned (Fig. 7), with the cores consisting of a regular intergrowths of hercynite and kamacite (sometimes with corundum) and rims of whitlockite or Cl-apatite, sometimes in assemblage with chromite. The outer portions of the cores pervasively carry rounded taenite inclusions. The outermost zone is a monomineral rim of olivine, which pseudomorphs marginal phenocrysts of pyroxene and olivine in the chondrule. The contours of the primary grains are easily discernible in the olivine rim. Figure 8 clearly displays tabular pyroxene grains near an HKO. A part of the grain remains unaltered, with the rest of the crystal (whose outlines are definitely visible in the rim) being completely replaced by newly formed olivine. The newly formed olivine rim is more ferrous (Fo$_{74-76}$) than the olivine in the chondrule (Fo$_{98}$). HKOs occasionally con-
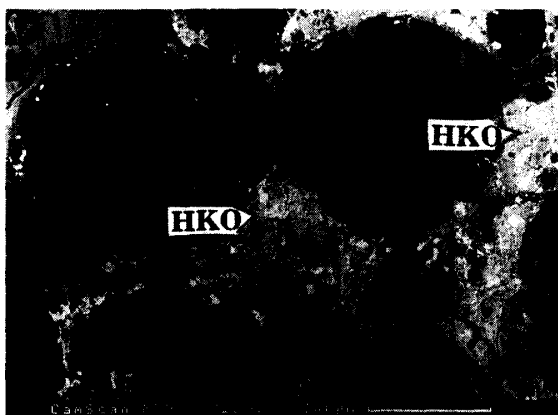
Fig. 2. BSE image of hercynite-kamacite aggre-
         gate (HKO) cementing silicate chon-
         drules.

Fig. 3. BSE image of chondrule-like hercynite-
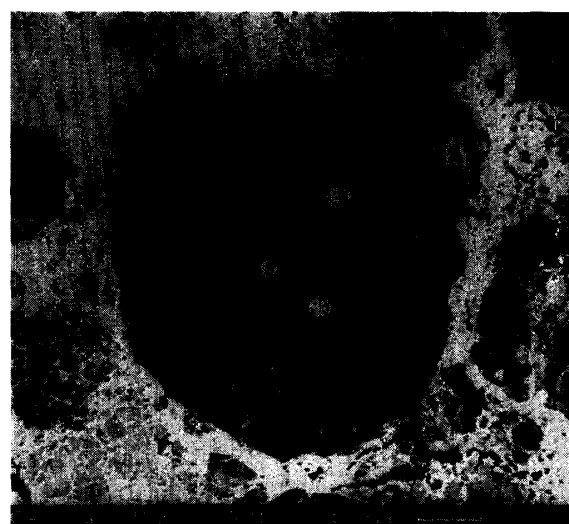   kamacite aggregate in the matrix.

Fig. 4. BSE image of abundant hercynite-
         kamacite droplets in a pyroxene-olivine
         porphyritic chondrule.

tain troilite and corundum (which occurs together with hercynite), and, in this case, the outer rim consists of troilite and pyroxene instead of olivine. HKO droplets in chondrules are less-susceptible to oxidation, unlike HKO in the matrix, which are intensely replaced by oxidized iron. The kamacite is replaced along both a network of submicron fractures, intersecting at 60°, and irregularly shaped veinlets, which cut hercynite-kamacite patches at random angles. The thickness of these veinlets varies broadly, up to the origin of fully replaced patches. The oxidized iron contains relict grains of corundum and hercynite, which are triangular or irregularly shaped (in patches of intense replacement). The iron oxidation in the chondrite is apparently secondary and partly obliterates the primary HKO texture in the matrix.

3. Mineral Chemistries

Nickel-iron is the principal HKO mineral (accounts for 85–90 vol% of HKO) and is mainly represented by kamacite and incidental taenite grains.
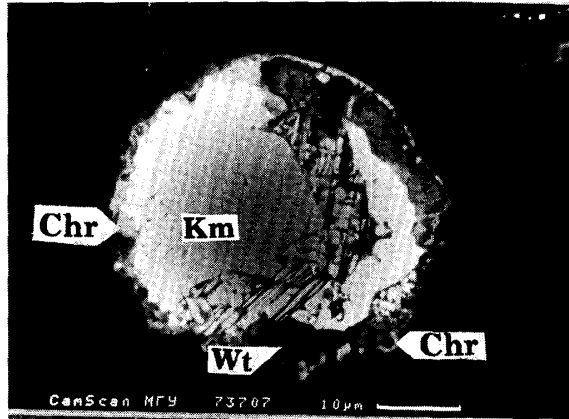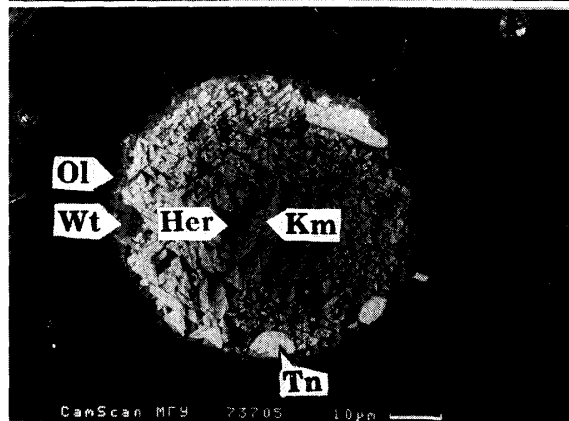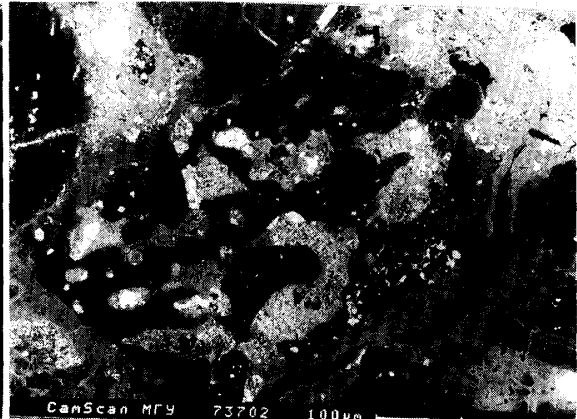
Fig. 5

Fig. 6

Fig. 7

Fig. 8

Fig. 5.   BSE image of a porphyritic hercynite-kamacite droplet in a pyroxene-olivine porphyritic chondrule (detail of Fig. 4). Interstices between euhedral kamacite crystals are filled with a fine-grained hercynite-kamacite aggregate. Km–kamacite, Chr–chrome spinel, Wt–whitlockite.

Fig. 6.   BSE image of hercynite-kamacite dumbbells in a porphyritic pyroxene-olivine chondrule.

Fig. 7.   BSE image of a zoned hercynite-kamacite droplet in a pyroxene-olivine porphyritic chondrule (fragment of Fig. 4). Km–kamacite, Her–hercynite, Wt–whitlockite, Tn–taenite, Ol–olivine.

Fig. 8.   BSE image of an olivine rim around HKO. Olivine (light gray) pseudomorphs marginal phenocrysts of pyroxene and olivine in the chondrule.

The kamacite occurs both in the chondrules and matrix HKO, and contains 3.5–5.9% Ni and 0.6–1.0% Co. Euhedral kamacite phenocrysts cemented by hercynite-kamacite material (Fig. 5) are lower in Ni (3.5–3.8% Ni) than the kamacite of the interstitial kamacite-hercynite aggregate (4.6–4.8% Ni). Kamacite of this aggregate and another HKO is cut by a network of submicron fractures intersecting at angles of 60°, along which the mineral is replaced by oxidized iron. By contrast, kamacite phenocrysts bear no such fractures. HKO of the matrix sometimes include elongated taenite grains (24–53% Ni and <0.5% Co), whose position is determined by the main arrays of fractures in kamacite. In HKO within chondrules, taenite of the same composition sometimes forms rounded inclusions along the whitlockite rim.

Spinels compose the second most abundant mineral group of HKO (accounts for 5–15 vol%). Table 1 presents analyses of spinels from the objects in question. The

Table 1.   Microprobe analyses (wt% of oxides) and chemical formulas (normalized to 4 oxygens) of spinels from hercynite-kamacite objects.

Oxide	Hercynites							Chromites			
	1*	2	3	4	5	6	7	8	9	10	11
	670	671	798	1359	758	907	1090	1092	1357	1358	1367
SiO_2	1.9	1.6	3.0	3.0	2.5	4.0	1.4	–	0.3	0.3	–
TiO_2	–	–	–	–	–	–	–	0.4	1.4	1.0	1.0
Al_2O_3	55.0	51.9	50.1	51.0	53.7	48.1	52.3	5.3	3.7	4.4	26.1
Cr_2O_3	–	–	–	–	–	0.5	–	53.2	59.6	58.8	35.4
V_2O_3	–	–	–	–	–	–	–	–	0.8	0.8	0.4
FeO	41.3	43.5	44.0	42.0	40.2	40.3	41.8	37.1	31.5	31.1	28.0
MnO	–	–	–	–	–	–	–	0.7	0.5	0.4	0.5
MgO	–	–	–	0.4	0.7	1.3	0.4	2.0	2.2	2.1	4.3
CaO	0.2	0.3	0.4	0.6	0.4	0.9	0.4	–	0.2	0.2	–
NiO	1.2	1.1	1.1	1.2	2.0	3.1	3.0	–	–	–	–
CoO	–	0.7	–	0.5	0.5	–	0.6	–	–	–	–
ZnO	–	–	–	–	–	–	–	–	–	1.0	4.2
Na_2O	0.4	0.7	0.8	1.1	–	1.2	–	1.5	–	–	–
K_2O	–	0.1	0.4	0.2	–	0.4	0.2	–	–	–	–
$MgAl_2O_4$	–	–	–	2.0	3.3	5.3	1.6	–	–	–	–
$FeAl_2O_4$	96.9	92.7	91.6	90.7	92.0	83.9	89.7	11.2	7.8	6.8	39.6
$(Ni,Co)Fe_2O_4$	2.9	4.2	2.7	4.2	4.7	8.0	7.6	–	–	–	–
$(Ni,Co)Al_2O_4$	–	–	–	–	–	–	1.1	–	–	–	–
$FeCr_2O_4$	–	–	–	–	–	–	–	65.7	73.3	72.5	24.2
$MgCr_2O_4$	–	–	–	–	–	0.7	–	10.3	11.8	11.3	20.8
$FeFe_2O_4$	0.2	3.0	5.7	3.1	–	2.1	–	9.6	0.8	1.9	1.1
$MnFe_2O_4$	–	–	–	–	–	–	–	2.2	1.5	1.2	1.5
Fe_2TiO_4	–	–	–	–	–	–	–	1.0	3.9	2.6	2.5
$ZnAl_2O_4$	–	–	–	–	–	–	–	–	–	2.5	9.9
$(V,Fe)_3O_4$	–	–	–	–	–	–	–	–	1.1	1.2	0.5

*Hercynites: 1–4 – from non-oxidized HKO; 5–7 – from oxidized HKO. Chromites: 8 – from untra-chondrule HKO; 9 – from matrix HKO; 10 and 11 – from pyroxene-olivine chondrule, core and rim accordingly.

analyses were accomplished by a microprobe equipped with an energy-dispersive analyzer (CamScan 4DV+Link AN 10000, an accelerating voltage of 15 kV, a sample current of 1.2×10^{-9} A, and an excitation area less than 3 µk) without measuring different iron valences. The end-member composition of the spinels was calculated by the method of SPIRIDONOV et al. (1989). As can be seen from the six-component diagram of HAGGERTY (1991) presented in Fig. 9, the HKO spinels are grouped into two compositional categories: one dominated by the hercynite end-member and the other by chromite, both characterized by low contents of ferric oxide, varying within similar limits.

The *hercynite-group spinels* develop systematic intergrowths with kamacite: a peculiar pattern resembling dissolution lamellar textures or fabrics originating during a nearly simultaneous crystallization of several phases. The hercynite always occurs at intersections of fractures in kamacite, and its morphology is apparently determined by the fracture network. In places, the hercynite looks like an interstitial mineral. In
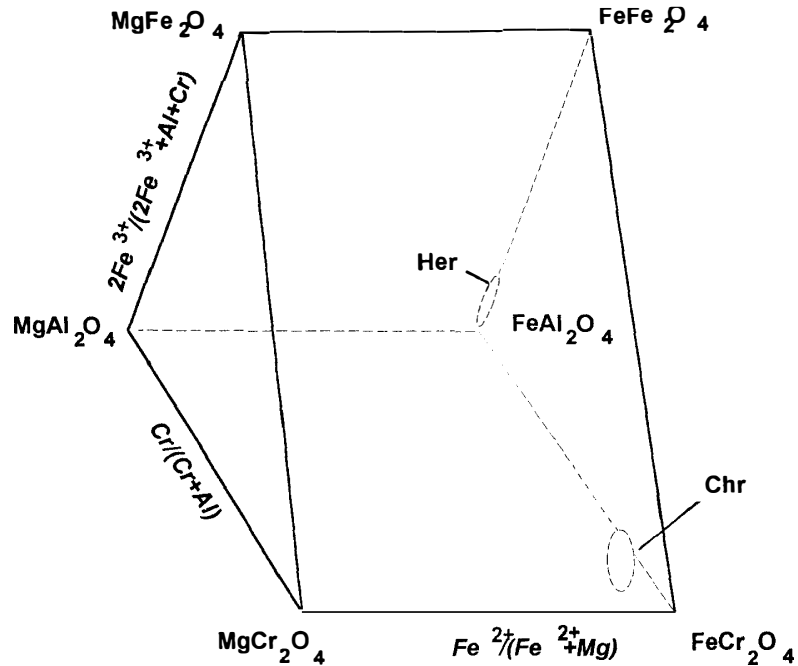
Fig. 9. Chemistries of HKO-spinels (Table 1) using spinel prism suggested by S. E. HAGGERTY (1991). The scale values represent the number of cations in tetrahedral and octahedral coordination for spinel formula based on 4 oxigens and 3 cations. 1–hercynites; 2–chrome spinels.
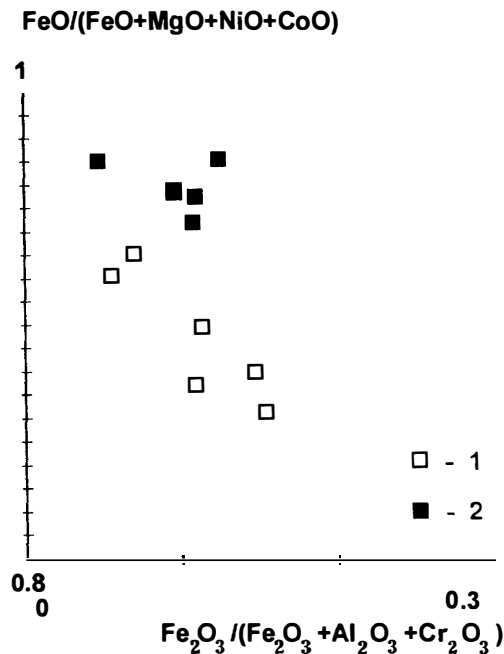

Fig. 10. Chemistries of HKO-hercynites (wt% of oxides) from non-oxidized (2) and oxidized (1) areas.

the plot of Fig. 10, the field of the hercynite group can be arbitrarily subdivided into two compositional regions, which have distinct contents of the hercynite component

and differ in their genesis. The hercynite with the maximum hercynite contents occurs in HKO both in chondrules and in the least oxidized portions of the matrix. The mineral forms triangular or trapezoidal grains up to 5–7 μm in size (Fig. 1, analyses 1–4 in Table 1), which show constant composition regardless of their position as inclusions in chondrules or in the matrix. The hercynite in oxidized patches either retains it triangular or trapezoidal morphology or, when the surrounding kamacite is strongly oxidized, becomes rounded up to relic-shaped in places of the strongest oxidation. As evident from Fig. 10, the hercynite from oxidized patches has, at similar ferric oxide contents, lower concentrations of the hercynite end member, which is partly replaced by trevorite and magnesian component (analyses 5–7 in Table 1). This fact provides evidence for that the secondary chondrite oxidation, regardless of its site, is overprinted on then-crystalline HKO, which invalidates the concept of a mechanical corundum entrapment. The occurrence of the trevorite component in the hercynite cannot be explained by the Ni and Fe incorporation from the surrounding kamacite: first, microprobe analyses were performed only in hercynite grains larger than the excitation area of the X-ray beam (5–7 μm and ~3 μm, respectively) and, second, no positive correlation was detected between the Ni and Fe contents in the hercynite analyses. The minor amount of Si, Ca, Na, and K, which normally do not occur in pure hercynite, seem to be caused by minor silicate admixture inevitably involved in the analyses. Nevertheless, the good reproducibility of the major element ratios allowed us to definitely ascribe to phase to hercynite.

Chromites occur in HKO both in the matrix and in chondrules but are not strictly governed by their textures. In intrachondrule HKO, the mineral is restricted to the peripheries, immediately at the boundary with the olivine rim, where it forms subhedral to rounded grains up to 3 μm (analysis 8 in Table 1). Chromites were detected in matrix HKO in incidental rounded grains up to 5 μm across.

The corundum occurs in triangular grains up to 8 μm with a persistent admixture of 3.5–18 wt% Fe but without Ni. This indicates that the corundum cannot be contaminated with the surrounding kamacite. Because such high Fe contents cannot be accommodated by the corundum lattice, the grains possibly contain tiny hercynite inclusions (which are involved in the analyses). The occurrence and textural position of the corundum in HKO typically depends on the presence of troilite. If HKO are devoid of sulfides, they rarely contain corundum, and the HKO are dominated by kamacite and hercynite. Conversely, in patches are abundant in troilite, corundum dominates over hercynite.

Phosphates are specific and ubiquitous minerals of HKO. The three phosphates detected in HKO are (Table 2) whitlockite, Cl-apatite, and Na-K phosphate; the minerals differ in their chemistry and textures. The whitlockite and Cl-apatite occur as rounded grains (up to 15 μm) in both the matrix and intrachondrule HKO. In the latter, these minerals are restricted to the contact with the chondrule material. Sometimes, they are zoned, with the cores consisting of whitlockite and the rims composed of Cl-apatite. The Na-K phosphate was detected only in the matrix HKO, in which it forms rounded grains up to 10 μm in diameter. The occurrence of tiny grains of Na-K phosphate in kamacite in ordinary chondrites H3 Dhajala and H4 Forest Vale was earlier described by PERRON et al. (1990), who demonstrated that the phosphate does not cor-

Table 2.   Average microprobe analyses (wt% of oxides) and chemical formulas (normalized to 24 oxygens) of phosphates from hercynite-kamacite objects.

Oxide	Whitlockite (5)*	Cl-apatite (4)	Na-K phosphate (5)	Cation proportions of phosphates
Na_2O	2.7	0.1	11.2	whitlockite -
K_2O	–	–	5.2	$-Na_{0.8}(Ca_{7.8}Mg_{0.81}Fe_{0.23})_{8.84}$
CaO	46.9	52.2	0.06	$P_{5.9}O_{24}\ Si_{0.02}\ Cl_{0.05}$
MgO	3.5	0.07	30.0	Cl-apatite -
FeO	1.7	2.1	4.7	$-Na_{0.04}(Ca_{9.81}Mg_{0.02}Fe_{0.30})_{10.13}$
MnO	–	–	0.6	$P_{5.89}O_{24}\ Cl_{1.75}$
P_2O_5	44.8	39.7	48.1	Na-K phosphate -
SiO_2	0.15	–	0.07	$-(Na_{3.16}K_{0.96})_{4.12}Ca_{0.01}$
Cl	0.2	5.88	–	$(Mg_{6.49}Fe_{0.57}Mn_{0.06})_{7.12}$
				$P_{5.91}O_{24}\ Si_{0.01}$

*Shown in parentheses are the numbers of analyses;– contents below the analytical threshold.

respond to any known mineral. In our case this phosphate is much higher in Na. The averaged chemical composition of this mineral is given in Table 2, and its idealized formula $Na_3K(Mg,Fe,Mn)_7(PO_4)_6$ suggests its relation to such rare phosphates as fillowite $Na_2Ca(Mn,Fe)_7(PO_4)_6$ (ARAKI and MOORE, 1981), johnsomervilleite Na_2CaMg_3 $(Fe,Mn)_4(PO_4)_6$ (LIVINGSTONE, 1980), and chladniite $Na_2CaMg_7(PO_4)_6$ (McCOY et al., 1994)—all of them having cell parameters and symmetry groups affiliating to the space group of fillowite. Chladniite was detected (McCOY et al., 1994), as a predominant phase, in the Carlton iron meteorite (IIICD) at the contact between silicate-bearing inclusions and nickel iron with schreibersite and accompanying olivine, pyroxene, plagioclase, and Cl-apatite. Plotted in the $MnO/(MgO + FeO + MnO) - MgO/(MgO + FeO + MnO) - CaO/(Na_2O + K_2O + CaO)$ diagram of Fig. 11 are phosphates of the fillowite structural group: fillowite, johnsomervilleite, and chladniite. As is apparent from the plot, the diversity of minerals in this group is determined by the isomorphism of elements in different structural sites: chladniite is a magnesian analog of fillowite, and johnsomervilleite is their ferrous-magnesian analog. McCOY et al. (1994) describe fillowite, johnsomervilleite, and chladniite by the same formula $Na_2CaX_7(PO_4)_6$, where X is Mg^{2+}, Fe^{2+}, and Mn^{2+}. The replacement of divalent Ca^{2+} by the sum of monovalent Na^+ and K^+ results in a phosphate phase with a formula analogous to that of the Na-K phosphate in HKO. Conceivably, the mineral is a Na-K Ca-free analog of fillowite. Unfortunately, the small size of its grains does not allow for its X-ray diffraction analysis. The occurrence of the unusual alkali phosphate in the HKO argues for the high alkalinity of these objects.

4.   Discussion of the Genetic Conditions

Hercynite-kamacite objects occur either in the matrix or, if in chondrules, solely in porphyritic pyroxene-olivine and olivine chondrules with magmatic textures and normal or complex zoning of their silicates. The general textural position of HKO and analysis of the textural phase relationships in HKO and variations of their mineral
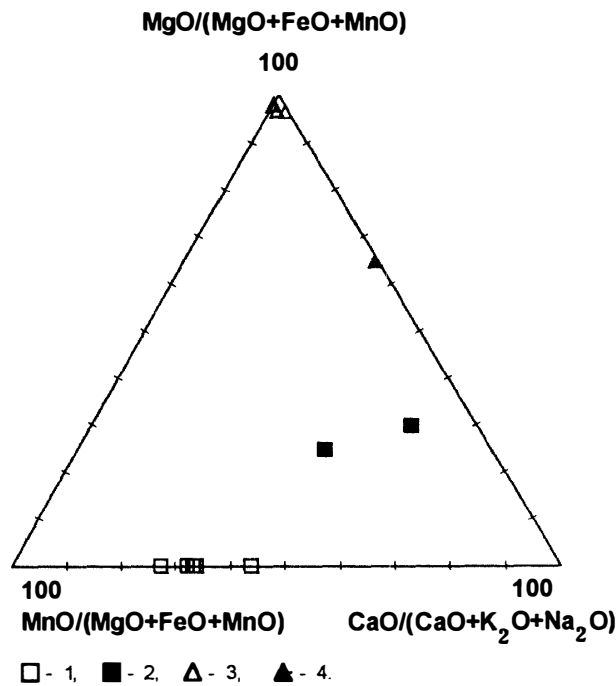
Fig. 11. Ternary plot showing the relationship between fillowite (1), johnsomervilleite (2), Na-K phosphate of HKO (3), and chladniite (4). Fillowite, johnsomervilleite, and chladniite have the general formula $Na_2CaX_7(PO_4)_6$, where X is Fe^{2+}, Mg^{2+}, or Mn^{2+} (ARAKI and MOORE, 1981; McCOY et al., 1994). The replacement of divalent Ca^{2+} by the sum of monovalent Na^+ and K^+ results in the Na-K phosphate in HKO.

composition provide convincing evidence for the magmatic genesis of these objects. This is apparent first and foremost from the specific morphology of intrachondrule HKO: these occur as drop-shaped inclusions, which sometimes coalesce to dumbbell-shaped bodies, i.e., typical features of only liquid systems. The melts of chondrules crystallized before the melt of the hercynite-kamacite objects did, and the latter was squeezed in the interstices of silicate chondrules. The magmatic genesis of intrachondrule HKO is also verified by the development of a porphyritic texture in some of them: interstices between euhedral kamacite crystals are filled with a fine-grained hercynite-kamacite aggregate produced from a residual melt. This also follows from the higher Ni contents of the kamacite in the aggregate and, thus, its lower crystallization temperature. It follows that the mechanism responsible for the separation of kamacite grains and hercynite-kamacite aggregates involves the sequential crystallization of kamacite and residual iron melt, which was rich in Al, P, and Cr. If the texture were subsolidus, the composition of the phenocrysts and aggregate would be the similar; the only possibility subsolidus texture is that of the interstitial aggregate, as it is discussed later. The composition of the HKO-forming melt can be inferred from the mineralogy of the aggregates: the occurrence of chrome spinels is suggestive of the elevated Cr content of the melt, ubiquitous phosphates point to its richness in P, and the occurrence of Na-K phosphate, which is atypical of the matrix assemblages, suggests the presence of alkalis. The richness of the hercynite-kamacite melt in fluids is corroborated by the metasomatic alterations of the crystalline material of chondrules

around HKO (olivine pseudomorphs after pyroxene in the outer olivine rims). It should be stressed here that the variations in the mineralogy and textures of HKO, whatever their position in chondrules or matrix, are determined by the local fluctuations in the contents of fluids: the presence of sulfur results in the hercynite-kamacite assemblage giving way to a paragenesis of corundum ($\pm$ hercynite) with troilite ($\pm$ kamacite). This brings about changes in the mineralogy of the outer HKO rim: troilite-pyroxene rims develop instead of monomineral olivine rims. Judging from the mineral assemblages, the transformations of the silicate material of chondrules under the effect of fluids equilibrated with HKO is similar to the processes of interaction between chondrules and the matrix of this chondrite and reflects the increasing oxygen activity (Zinovieva et al., 1996a). The interstitial position of HKO, occurrence of HKO veinlets cutting silicate chondrules, and their richness in alkalis and phosphates are indicative of the lower viscosity of the HKO melt compared to the silicate melt of chondrules and the lower liquidus temperature of the former. During the cooling and partial crystallization of the silicate melt, the Al-Fe melt becomes reactive with respect to the silicate melt and it brings about the above-mentioned metasomatic alterations in the near-boundary zones.

An interesting fact of principal importance is the occurrence, although very rare, of hercynite-kamacite veinlets cutting porphyritic olivine-pyroxene chondrules and the interstitial position of a part of the matrix HKO, cementing chondrules. This indicates that the HKO formed in parental body. Although of the hercynite-kamacite melt in the matrix and the hercynite-kamacite veinlets (cutting the olivine-pyroxene chondrules) might be explained by impact melting, neither the olivine and pyroxene of the adjacent chondrules nor silicate fragments in the fine-grained matrix show evidence of impact metamorphism, and this contradicts the concept of impact melting. At the same time, the separation textures of the magnesian-silicate and Al-Fe material in chondrules apparently point to the liquid immiscibility of the homogeneous melt of chondrules, which split into originally equilibrated silicate and fluid- and metal-rich (with Al and, rarely, S) liquids. Taking into account that the textures, mineralogy, and mineral chemistries of HKO in chondrules and in the matrix of the chondrite are absolutely identical, it is difficult to perceive that objects of similar texture and mineral composition in chondrules and in the matrix of a single chondrite were produced by principally different processes.

Interestingly, neither reduced nor oxidized (corundum and hercynite) Al compounds have been detected in kamacite of ordinary chondrites, although Si, Cr, and P typically occur in kamacite of carbonaceous and ordinary chondrites (Perron et al., 1992; Zanda et al., 1994). In kamacite from chondrites of low petrological types (types 2 and 3.0), reduced forms are dissolved in the metallic phase. A negative correlation of Cr, Si, and P components in kamacite with the fayalite mole fraction of the olivine led authors to conclude that the metal was in equilibrium with the silicate in the chondrules.

We were the first to discover natural Al-rich phases in kamacite. The textures of kamacite aggregates crossed by a network of submicron fractures, which are now filled with oxidized iron and intersect at angles of 60° can be interpreted (Bochvar, 1956) either as the result of deformations or as a textural analog of Widmanstatten patterns.

The final choice between these mechanisms can be made on the basis of textural relationships between kamacite and hercynite in HKO included in chondrules in that kamacite phenocrysts bear no fractures specific of interstitial kamacite-hercynite aggregates and, hence, the whole texture is unlikely to be deformation-related.

Textures analogous to Widmanstatten patterns are well known (BOCHVAR, 1956; NATANOV, 1956) in metallurgy and are caused by rapid supercooling of a steel melt, when strong stress appears in crystals of the alloy under the action of which the transformation is oriented only along certain planes and directions in crystals of the initial exsolving phase. This results in the origin of markedly acicular or more specifically, tabular textures. Certain portions of the newly formed phase are set at definite angles to one another, for example, ubiquitous pairs of platelets intersecting at 60 and 120°.

Also known in metallurgy are magnetic Fe-Al-Ni alloys (Bochvar, 1956), which compose a homogeneous solution at high temperatures, which decomposes, in castings (particularly as a result of supercooling during chilling), into two solid solutions with analogous structures but different cell parameters.

The observed apparent crystallographic orientation in the texture of the HKO (hercynite and corundum crystals are regularly oriented relative to kamacite) can be interpreted either as a granophyric texture (kamacite-hercynite intergrowths during their simultaneous crystallization) or a texture of dissolution and later oxidation of the Al-bearing alloy. It is difficult to solve this problem unambiguously. Fe-Al alloys involve a number of phases, in the Fe-rich region, that differ in magnetic properties and crystal structures (VOL, 1959). One of them is Fe_3Al, which forms from a solid solution of Al in Fe at decreasing temperature. Also known in metallurgy is the ability of Al, Cr, and Si to form a compact oxide superficial film, which makes the steel more resistant to oxidation (NATANOV, 1956). This mechanism could explain the weaker oxidation of kamacite in HKO (in Yamato-82133) than that in the matrix; the matrix kamacites not accompanied by alumina. Then, oxidation of the Al-bearing HKO phase itself would produce hercynite and/or corundum.

Comparing estimates, based on the assemblage of Si, Cr, Fe, and troilite (PERRON et al., 1992; ZANDA et al., 1994), of the redox conditions at which chondrites of low petrological types form with a $\mu O_2-\mu S_2$ diagram (Fig. 12) showing formation of oxides, sulfides, and water-free silicates from elements at a temperature of 1200 K and standard pressure (MARAKUSHEV and BEZMEN, 1972), one can conclude that Al should be present in the system in the form of hercynite and corundum. Reduced Al forms need more reduced conditions for their origin. However, it is pertinent to note that the stability fields of native elements expand with increasing temperature. The simultaneous occurrence of hercynite and corundum in iron is a usual association, which was studied in detail in ferrous metallurgy. It was detected in Al-rich refractories after their interaction with steel (IVANOV, 1953). Moreover, MAMYKIN and ZLATKIN (1953) determined that corundum occurs in steel itself as a detrimental impurity and forms at the expense of native aluminum, which is added to steel for its deoxidation. The Fe-Al-O diagram (ATLAS and SUMIDA, 1974) confirms the existence of the assemblage of native iron, corundum, and hercynite even at moderate (1000°C) temperatures.

The presence of HKO in the same mineral assemblage and its definite textural position in the chondrite indicates that, whatever the mode of Al occurrence in the
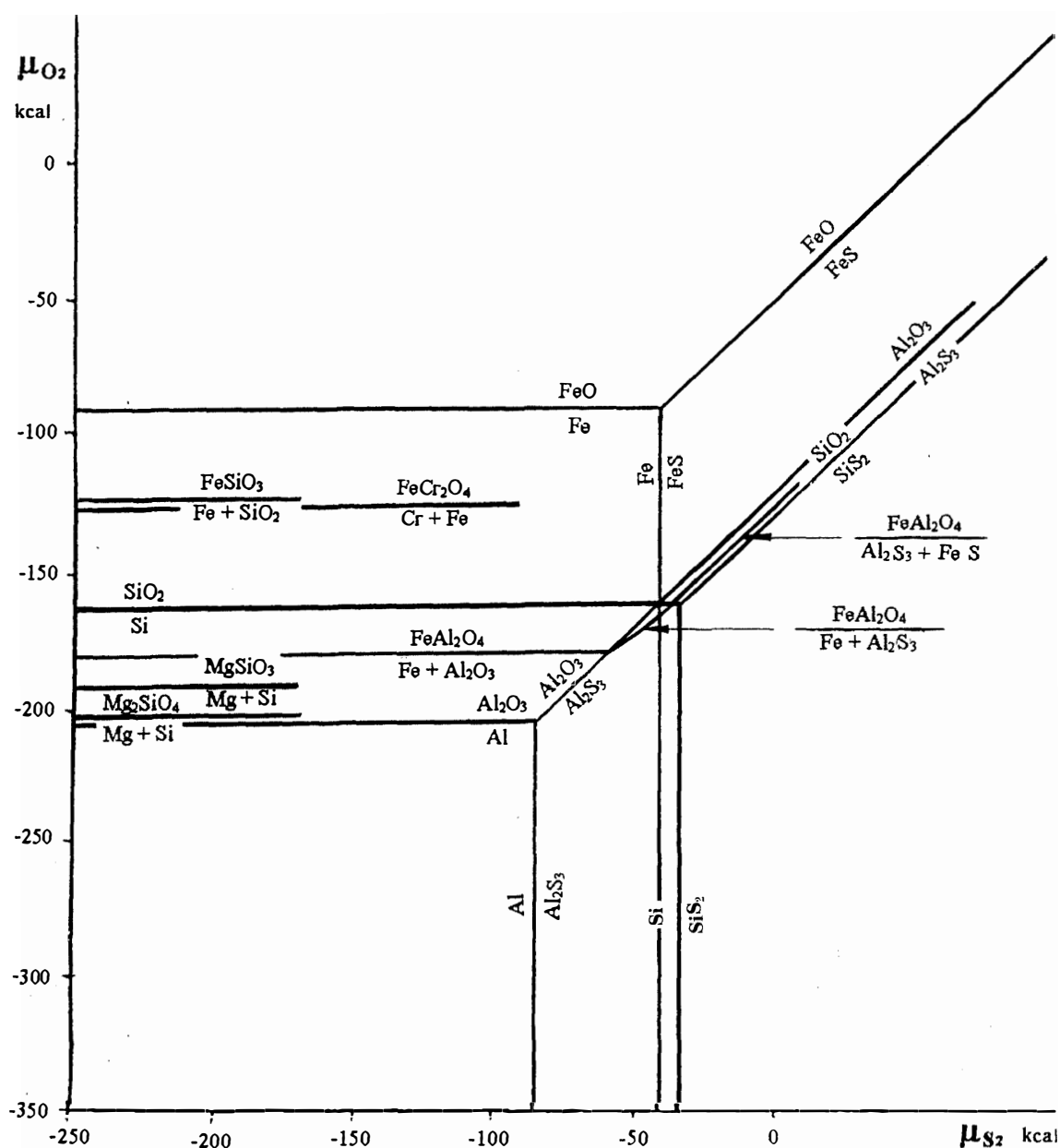
Fig. 12. Equilibria of metals with oxides, sulfides, and silicates at a temperature 1200 K and standard pressure.

metal phase, there was an Al-rich Fe-Ni melt, which immiscibly split from the chondrule melt. The former crystallized after the chondrule silicate melt and caused metasomatic transformations of the already-solid silicate material.

Acknowledgments

References

ARAKI, T. and MOORE, P. B. (1981): Fillowite, $Na_2Ca(Mn,Fe)_7^{2+}(PO_4)_6$: Its crystal structure. Am. Mineral., **66**, 827–842.

ATLAS, L. M. and SUMIDA, W. K. (1974): Minerals: Reference Book of Phase Diagrams. Moscow, Nauka Press, 91.

BOCHVAR, A. A. (1956): Phizicheskaya Metallurgiya (Physical Metallurgy). Moscow, Chem.-Tsvet.-Met. Press, 495 p.

HAGGERTY, S. E. (1991): Oxide mineralogy of the upper mantle. Rev. Mineral., **25**, 357–415.

IVANOV, B. V. (1953): About the problem of a mineral composition of refractories. Voprosy Petrografii i Mineralogii (Problems of Petrography and Mineralogy), II. Moscow, Nauka Press, 358–366 (in Russian).

LIVINGSTONE, A. (1980): Johnsomervilleite, a new transition-metal phosphate mineral from the Loch Quoich area, Scotland. Mineral. Mag., **43**, 833–836.

MAMYKIN, P. S. and ZLATKIN, S. G. (1953): Non-metallic inclusions in metal in dependence on composition and properties of refractories. Voprosy Petrografii i Mineralogii (Problems of Petrography and Mineralogy), II. Moscow, Nauka Press, 271–280 (in Russian).

MARAKUSHEV, A. A. and BEZMEN, N. I. (1972): Termodinamika Sulfidov i Okislov v Sviazi s Problemami Rudoobrazovania (Thermodynamics of Sulfides and Oxides in Accordance with Ore Formation Problems). Moscow, Nauka press, 229 p.

McCOY, T. J., STEELE, I. M., KEIL, K., LEONARD, B. F. and ENDREß, M. (1994): Chladniite, Na_2CaMg_7 $(PO_4)_6$: A new mineral from the Carlton (IIICD) iron meteorite. Am. Mineral., **79**, 375–380.

NATANOV, B S. (1956): Metallovedeniye (Physical Metallurgy). Moscow, Chem.-Tsvet.-Met. Press, 344 p.

PERRON, C., BOUROT-DENISE, M., PELLAS, P. and MARTI, K. (1990): Si-, P-, Cr-bearing inclusions in Fe-Ni of ordinary chondrites. Meteoritics, **25**, 398–399.

PERRON, C., ZANDA, B., BOUROT-DENISE, M. and MOSTEFAOUI, S. (1992): Bishunpur and Semarkona: New clues to the origin of inclusions in metal. Meteoritics, **27**, N3, 275.

SPIRIDONOV, E. M., KOROTAEVA, N. N. and LADYGIN, V. M. (1989): Chromian spinels, titanomagnetite and ilmenite of island arc volcanoes from Gornyi Crimea. Vestnik Moskovskogo Universiteta, Seria Geologiya (J. Moscow Univ., Geol.), **6**, 37–55 (in Russian).

VOL, A. EY. (1959): Stroyeniye i Svoyistva Dvoyinykh Metallicheskikh Sistem (Composition and Properties of Double Metallic Systems). Moscow, Phyzmatgiz Press, 755 p.

YANAI, K. and KOJIMA, H., comp. (1995): Catalog of the Antarctic Meteorites. Tokyo, Natl Inst. Polar Res., 230 p.

ZANDA, B., BOUROT-DENISE, M., PERRON, C. and HEWINS, R. H. (1994): Origin and metamorphic redistribution of silicon, chromium, and phosphorus in the metal of chondrites. Science, **265**, 1846–1849.

ZINOVIEVA, N. G., MITREIKINA, O. B. and GRANOVSKY, L. B. (1995): Specific pyroxene-olivine chondrules of the Yamato-82133 (H3) chondrite: Evidence of the evolution of redox conditions during the chondrule formation. Antarctic Meteorites XX. Tokyo, Natl Inst. Polar Res., 288–290.

ZINOVIEVA, N. G., MITREIKINA, O. B. and GRANOVSKY, L. B. (1996a): Interaction between chondrules and matrix in chondrites: Evidence from the Yamato-82133 (H3) chondrite. Antarctic Meteorites XXI. Tokyo, Natl Inst. Polar Res., 219–221.

ZINOVIEVA, N. G., MITREIKINA, O. B. and GRANOVSKY, L. B. (1996b): Occurrence of hercynite in the ordinary chondrite Yamato-82133 (H3). Lunar and Planetary Science XXVII. Houston, Lunar Planet. Inst., 1499–1500.

ZINOVIEVA, N. G., MITREIKINA, O. B. and GRANOVSKY, L. B. (1996c): Origin mechanism of hercynite-kamacite objects: Evidence for liquid immiscibility phenomena in the Yamato-82133 (H3) ordinary chondrite. Antarctic Meteorites XXI. Tokyo, Natl Inst. Polar Res., 222–224